Accurate measurements of Optical Turbulence with Sonic- anemometers

2015 J. Phys.: Conf. Ser. 595 012036

(http://iopscience.iop.org/1742-6596/595/1/012036)

Accurate measurements of Optical Turbulence with Sonic-anemometers

T Travouillon[1], A Otarola[1], S Els[2], R Riddle[3], M Schöck[1], W Skidmore[1], D Bibb

[1]Thirty Meter Telescope, 111 South Arroyo Parkway, Pasadena, 91105 CA, USA
[2]Gaia DPAC, c/o ESAC
[3]California Institute of Technology, 1200 E. California blvd, Pasadena, 91125 CA, USA

E-mail: tonyt@caltech.edu

Abstract. The minimization of optical turbulence in and around the dome is key to reach optimum performance on large telescopes equipped with adaptive optics. We present the method and preliminary results of in-situ measurements of optical measurements made using sonic-anemometers. We show the impact of correcting the raw data for aliasing, path averaging, pulse sequence delays and Taylors' hypothesis. Finally, we highlight the occurrence of non-Kolmogorov turbulence which complicates the quantitative impact of the measurements on the telescope's resolution.

1. Introduction

The site testing campaign for the Thirty Meter Telescope (TMT) took place between 2003 and 2008 [1]. A minimum of 2 years of data were recorded at 5 sites: Cerros Armazones, Tolar and Tolonchar in Chile, San Pedro Martír in Mexico and finally Maunakea in Hawaii which ended up being selected for the construction of TMT. The resulting data set includes an array of key parameters including meteorological parameters, turbulence, all-sky images, atmospheric transparency and sky brightness. These data have been made publically available and accessible online (www.sitedata.tmt.org).

Several instruments used during this campaign are seen as having a useful purpose during the operation of the telescope as well. One of them, a CSAT3 model sonic-anemometer was used at every site gathering temperature and wind velocity data from the 7m tower of the DIMM telescope. Thanks to the high cadence of the measurements (60Hz), it is in principle possible to use the wind and temperature to calculate the turbulence parameter C_n^2. Such capability makes this instrument ideal for *in-situ* measurements of turbulence inside an observatory. In such an environment, remote sensing is impractical and inadequate for highly localized measurements. Scintillometers for example, measure the turbulence over a given path instead of at a specific location. The only instrument commonly used for making pinpointed measurements of optical turbulence is the thin-wire microthermal sensor. This instrument is commonly used balloon-born to measure turbulence profiles of the atmosphere, but when used at a stationary location, its fragile construct means that it breaks under tough meteorological conditions. A sonic-anemometer, on the other hand is built to handle any conditions due to its metal frame and its lack of moving parts.

The goal is to use the sonic-anemometers operated during the TMT site testing campaign around key locations around the dome of the telescope to measure the turbulence field and minimize this turbulence to obtain the best possible on-sky resolution. In this paper, we present the initial work made to transform the sonic-anemometer data into accurate turbulence measurements. We summarize how the raw temperature and wind velocity data were combined and corrected to obtain time series of the turbulence figure of merit: C_T^2. We also open a discussion on an observation made during the analysis of these data: non-Kolmogorov turbulence.

2. Sonic-Anemometer data

While the completion of the construction of TMT is still a few years away, testing the CSAT3 suitability can be done on existing data. A very large sample of raw temperature and wind velocity data was sampled at 60Hz, totaling to approximately 35GB per site, and is available for the five sites studied in the campaign. The sonic-anemometers were located at a height of 7m above the ground, attached to the structure of the DIMM telescope tower. They were installed upwind on an extended arm to keep the head of the sensor 1.5m away from the dome structure. In addition to this setup, 30m towers were installed on Cerro Armazones and Cerro Tolonchar and three anemometers were installed at 10, 20 and 30m to obtain a vertical profile of the site's weather conditions. In this paper however, we will focus on a small subset of the data using the first 3 months of the Maunakea dataset. As the next section will show, the data reduction is computer intensive and this smaller dataset allows us to more easily test the analysis routines and draw initial conclusions on how to proceed with the full analysis.

To understand the processing of the raw data described in the next section, it is important to know the basics of the instrument in question. The CSAT3 uses three pairs of acoustic transducers with the geometrical characteristics shown in Figure 1. A sonic pulse is sent from one transducer to its opposing counterpart. The temperature θ, often referred to as "sonic temperature", is deduced from its simplified relationship to the speed of sound:

$$c_{sound} = (331.3 + 0.606\,\theta) \quad (1)$$

This temperature is therefore an average of the temperature inside the cylindrical beam the pulse travels through. Each pair of transducer takes turn to go through a cycle of sonic emission/reception to give for each a wind speed along the line of the transducers pair. From these and using simple geometry, the *x*, *y* and *z* component of the wind velocity can also be calculated.

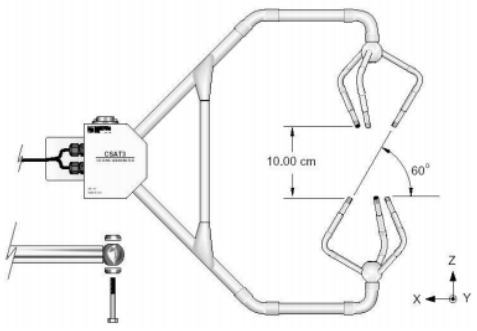

Figure 1. Visual representation of the CSAT3 sonic-anemometer.

Sixty times per second a sonic temperature and three wind speed components are measured and recorded by the instrument along with a quality flag. This quality flag is used to identify times when the sonic beam was blocked (by ice for example) or simply of poor accuracy due to a low signal to

noise ratio. Such data were discarded all together from our analysis. Finally the data are divided into 2mn blocks from which the temperature power spectrum $S_T(f)$ and the mean wind speed U are calculated. It is from these parameters that the turbulence can be calculated:

$$C_T^2 = 13.67 S_T(f) f^{5/3} U^{-2/3} \quad (2)$$

In reality however, it is important to carry out some corrections to the temperature power spectrum before applying it to the above formula. In the section below, we describe and estimate the different types of correction that are required to transform the sonic-anemometer's date into real single point measurements of temperature and wind velocity. It is with this corrections that we can aim for the most accurate turbulence measurements possible.

3. Data correction

3.1. Aliasing and white noise

With a limited sampling speed of 60Hz, the range of measurement is limited to a Nyquist frequency of half this value and subjected to aliasing effects like any other digital sampling. The energy above this frequency is however folded back into the observed range which is visible in a raw power spectrum in the form of an "uptail" in the high frequency end of the spectrum. The corrected power spectrum is deduced from the aliased power spectrum $S^a(f)$ through the relation:

$$S(f) = S^a(f) / \sum_{m=-\infty}^{\infty} H(f_m) \left(\frac{f_m}{m}\right)^{-5/3} \quad (3)$$

where $f_m = |f + 2mf_N|$ and $H(f)$ is the attenuation caused by the processes described in the subsections below. Figure 2 shows the visual effect of de-aliasing the power spectrum, removing the folded energy and linearizing the power spectrum in the log space.

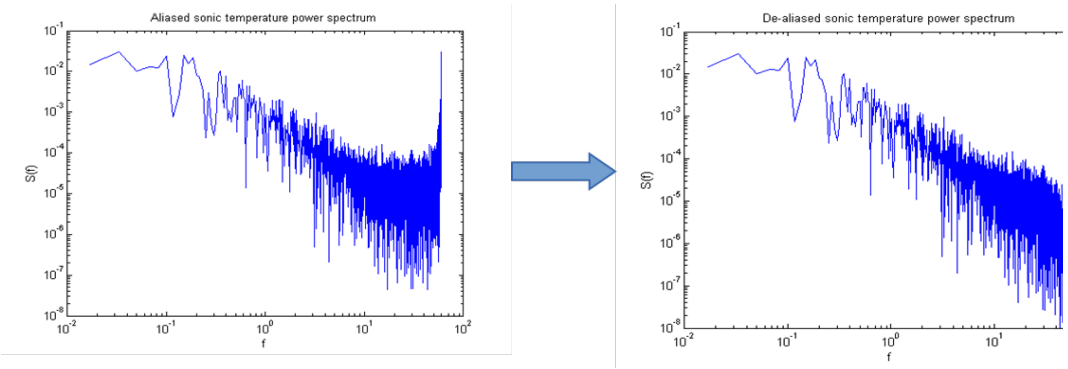

Figure 2. Example taken from our analysis of power spectrum de-aliasing.

From this de-aliased spectrum, white noise can easily be removed since the CSAT3's noise is independent of sampling rate and approximately equal to $\sigma = 0.004^{\circ}C$. A constant value of σ^2/f_N is therefore subtracted from the power spectrum.

3.2. Sonic path-averaging

As visible in Figure 1, the sonic pulse has to traverse a volume of air to go from the emitting transducer to its receiving counterpart. The size of this path is not negligible with a vertical distance of

10cm and therefore has the effect of averaging over that volume. This averaging, which affects both temperature and wind speed measurements, is aggravated by the fact that the anemometer needs to combine the data from the three paths. The temperature averaged over a path p is related to the punctual temperature at the centre of the path,x_0, following:

$$\tilde{T}(x_0, p) = \frac{1}{p}\int_{-p/2}^{p/2} T(x_0 + s)ds \tag{3}$$

The mathematical leap to the Fourier space, which is described in [2], leads to a transfer function H^p which must be applied to both temperature and wind speed power spectrum.

3.3. Pulse sequence delays

A full cycle of measurements with the CSAT3 requires 6 pulses: one in each direction for each pair of transducers. This sequence takes a total of 13.4msec during which the turbulence has not been stationary. This effect studied initially by Larsen et al. [3] and updated by Nielsen and Larsen [4] constitutes an attenuation and a cross contamination of the temperature and wind velocity spectra. For example, the temperature measurement made by the CSAT3, T_S, is an average of the measurements of the three paths and is related to the true sonic temperature, T_{sv}, via:

$$T_S = \frac{1}{6}\sum_{j=1}^{6} T_{sv}(t_j) + \frac{a}{6}[w_a(t_1) - w_a(t_2) + w_b(t_3) - w_b(t_4) + w_c(t_5) - w_c(t_6)] \tag{4}$$

where w is the wind speed along the three paths a, b and c of the instrument. Its Fourier transform leads to a correction factor dependent on spectra and co-spectra of both temperature and wind velocity. The temperature power spectrum is therefore attenuated by a factor H^τ which is used in the net spectral correction.
After the temperature power spectrum has been de-aliased and white noise was removed, a net correction that takes consideration of both pulse delay and path averaging:

$$\begin{aligned} S_T(f) = S_{Tcorrected}(f) &\sum_{m=-\infty}^{\infty} H_T^p(\omega_m/U)H_T^\tau(\omega_m)\left(\frac{f_m}{f}\right)^{-\frac{5}{3}} \\ &+S_{wa}\sum_{m=-\infty}^{\infty} H_{wa}^p(\omega_m/U)H_{wa}^\tau(\omega_m)\left(\frac{f_m}{f}\right)^{-\frac{5}{3}} + \cdots \\ &+Co_{waT}\textstyle\sum_{m=-\infty}^{\infty}[H_{wa}^p\left(\frac{\omega_m}{U}\right)H_T^p\left(\frac{\omega_m}{U}\right)]^{1/2}H_{waT}^\tau(\omega_m)\left(\frac{f_m}{f}\right)^{-\frac{57}{3}} + \cdots \end{aligned} \tag{5}$$

where $\omega = 2\pi f$ and the derivation of the attenuations factors can be found in the references above.

3.4. Taylor's hypothesis

The final spectrum is corrected for Taylor's hypothesis which is assumed above. This is done out of completeness only and not necessary for our data, since we found it to only contribute a correction of about 1%, Wyngaard and Clifford [5] show that the ratio of the measured to real power spectrum is:

$$\frac{S^m}{S} = 1 - \frac{1}{9}\frac{\overline{u'u'}}{\bar{U}^2} + \frac{1}{3}\frac{\overline{v'v'}}{\bar{U}^2} + \frac{1}{3}\frac{\overline{w'w'}}{\bar{U}^2} \tag{6}$$

where u, v and w are the wind speed along the x, y and z as labelled in Figure 1.

4. Results

As mentioned earlier, applying all the corrections to a power spectrum is quite computer intensive and the purpose of testing it on a subset of the data is to test the software and get an idea for the size of the correction. If the effect is found to be very small, the correction can simply be ignored and if the effect is systematic, it can at least be simplified. With the wide variations of C_T^2 that can be encountered throughout a night of measurement, a random variation of 5% could, for example, easily be considered acceptable. So the first obvious comparison is that of the corrected C_T^2 versus its raw

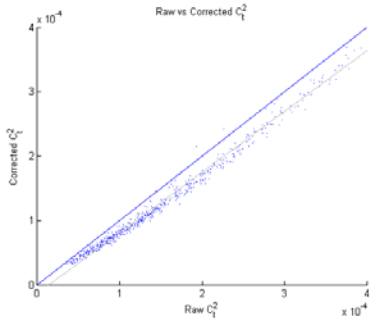

Figure 3. Scatter representation of the corrected and raw C_T^2.

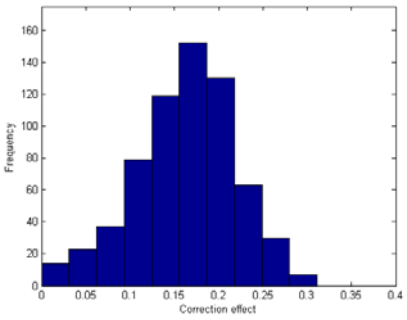

Figure 4. Statistical distribution of the correction factor in percentage.

counterpart.

Figures 3 and 4 show the effect of the correction on the data subset. The correction systematically decreases the value of the measured turbulence with a mean correction corresponding to a 16% decrease. The scatter in the correction is also small as it never exceeds 30%. The line of best fit, shown in grey on Figure 3 as a slope of 0.95, meaning that the intensity of the turbulence has little effect on the size of the correction. Looking at the data a bit deeper, we can see that the parameter affecting the correction is, not surprisingly, the wind speed since it impacts both the path averaging and pulse delay elements of the correction (i.e. a higher wind speed moves an air volume further between each pulse). Figure 5 shows an almost systematic increase of the correction factor with wind velocity. This relationship is even linear enough to be used as a crude correction method (the dip between 2 and $4m.s^{-1}$ is most likely due to low number statistics) and shows that inside an observatory, where the wind speeds will be low, the correction may even have a small effect

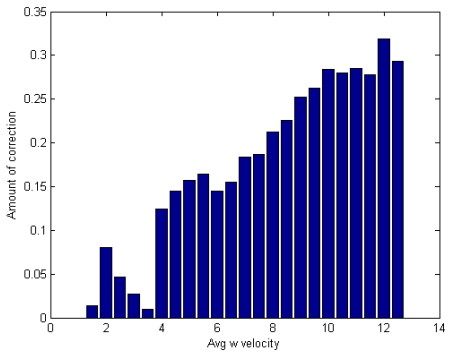

Figure 5. Wind velocity dependence of the correction factor.

5. The problem of non-Kolmogorov turbulence and conclusion

The analysis of these data had the unintended consequence of attracting our attention to a more fundamental problem. Equation 2 assumes a Kolmogorov turbulence spectrum, which has a frequency dependence with a -5/3 power law. In reality, however, the power spectrum does not always have such a frequency dependence. Leaving aside the practical difficulties and choices that are necessary to fit a power law to a noisy spectrum, we found that not only was the slope of the power spectrum in log space not always equal to the expected -5/3 but had some systematic variations with the time of the day (see figure 6). The nature of these variations are likely linked to the stability of the turbulence and its interaction with the ground and physical features. With an instrument only 7m from the ground, and in even closer proximity with a metallic tower, it is not surprisingly to find turbulence conditions that are not fully developped. But the question persists: as the intended purpose is to use this instrument inside and around an observatory, how does one measure non-Kolmogorov turbulence and translate the data to a quantity that can then be used to estimate the telescope loss of resolution contributed by this dome turbulence?

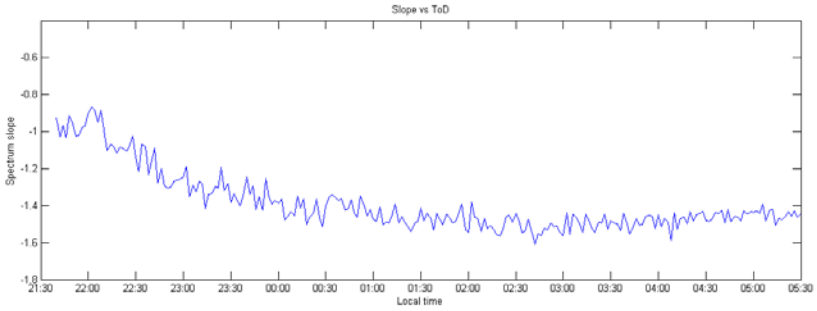

Figure 6. Slope of the power law (in log-space) as function of the time of the day. The instrument was only operated in night time but the data suggest that the turbulence conditions only approach Kolmogorov a few hours after sunset.

Acknowledgment

We would like to thank Tom Horst and Steve Oncley for establishing the theoretical framework around which this work is based. The TMT Project gratefully acknowledges the support of the TMT collaborating institutions. They are the Association of Canadian Universities for Research in Astronomy (ACURA), the California Institute of Technology, the University of California, the National Astronomical Observatory of Japan, the National Astronomical Observatories of China and their consortium partners, and the Department of Science and Technology of India and their supported institutes. This work was supported as well by the Gordon and Betty Moore Foundation, the Canada Foundation for Innovation, the Ontario Ministry of Research and Innovation, the National Research Council of Canada, the Natural Sciences and Engineering Research Council of Canada, the British Columbia Knowledge Development Fund, the Association of Universities for Research in Astronomy (AURA), the U.S. National Science Foundation and the National Institutes of Natural Sciences of Japan.

References

[1] Schöck M et al. 2009 *Thirty Meter Telescope Site Testing I: Overview* Publ. Astr. Soc. Pac. 121 (878) pp 384-395
[2] Horst T W, and Oncley S P 2006 *Corrections to inertial-range power spectra measured by*

CSAT3 and Solent sonic anemometers, 1. Path-average errors. Boundary Layer Meteorology 119 pp 375--395.

[3] Larsen S E, Edson J B, Fairall C W and Mestayer P G 1993 *Measurement of temperature spectra by a sonic anemometer* J. Atmos. Oceanic Tech. 10 pp 345–354.

[4] Nielsen M and Larsen S E 2002 *The influence of pulse–firing delays on sonic anemometer response characteristics* 15th AMS Conference on Boundary Layers July 15-19, 2002, Waginingen, The Netherlands, pp 436-439.

[5] Wyngaard J C, Clifford S F 1977 Journal of Atmospheric Sciences vol. 34 Issue 6 pp 922-929